doi:10.1093/brain/awm118 *Brain* (2007), **130**, 1942–1956

Angiogenesis is associated with blood–brain barrier permeability in temporal lobe epilepsy

Valérie Rigau,[1,2,3,*] Mélanie Morin,[1,2,*] Marie-Claude Rousset,[1,2] Frédéric de Bock,[1,2] Aurore Lebrun,[1,2] Philippe Coubes,[1,2,4] Marie-Christine Picot,[4] Michel Baldy-Moulinier,[4] Joël Bockaert,[1,2] Arielle Crespel[1,2,4] and Mireille Lerner-Natoli[1,2]

[1]Centre National de la Recherche Scientifique UMR5203, Université Montpellier I, Université Montpellier 2, F34094 Montpellier, [2]Institut de la Santé et de la Recherche Medicale U661, F34094 Montpellier, [3]CHU, Laboratoire d'Anatomie et Cytologie Pathologiques, F34295 Montpellier and [4]CHU, Unité d'Epileptologie, F34295 Montpellier

*These authors contributed equally to this work.

Correspondence to: Mireille Lerner-Natoli, PhD, Institut de Génomique Fonctionnelle, 141 rue de la Cardonille, 34094 Montpellier Cedex 5, France
E-mail: mireille.lerner-natoli@igf.cnrs.fr

Previous studies from our group, focusing on neuro-glial remodelling in human temporal lobe epilepsy (TLE), have shown the presence of immature vascular cells in various areas of the hippocampus. Here, we investigated angiogenic processes in hippocampi surgically removed from adult patients suffering from chronic intractable TLE, with various aetiologies. We compared hippocampi from TLE patients to hippocampi obtained after surgery or autopsy from non-epileptic patients (NE). We quantified the vascular density, checked for the expression of angiogenic factors and their receptors and looked for any blood–brain barrier (BBB) leakage. We used a relevant model of rat limbic epilepsy, induced by lithium-pilocarpine treatment, to understand the sequence of events. In humans, the vessel density was significantly higher in TLE than in NE patients. This was neither dependent on the aetiology nor on the degree of neuronal loss, but was positively correlated with seizure frequency. In the whole hippocampus, we observed many complex, tortuous microvessels. In the dentate gyrus, when the granular layer was dispersed, long microvessels appeared radially orientated. Vascular endothelial factor (VEGF) and tyrosine kinase receptors were detected in different types of cells. An impairment of the BBB was demonstrated by the loss of tight junctions and by Immunoglobulines G (IgG) leakage and accumulation in neurons. In the rat model of TLE, VEGF over-expression and BBB impairment occurred early after status epilepticus, followed by a progressive increase in vascularization. In humans and rodents, angiogenic processes and BBB disruption were still obvious in the chronic focus, probably activated by recurrent seizures. We suggest that the persistent leakage of serum IgG in the interstitial space and their uptake by neurons may participate in hypoperfusion and in neuronal dysfunction occurring in TLE.

Keywords: temporal lobe epilepsy; angiogenesis; vascular endothelial growth factor; blood-brain barrier disruption; IgG leakage

Abbreviations: AVM = arterio-venous malformation; CRYPTO = cryptogenetic; DG = dentate gyrus; DGL = dentate granular layer; DNET = dysembryoplastic neuroepithelial tumour; DYSP = focal dysplasia; Ext-TLE = external temporal lobe epilepsy; FH = fissura hippocampi; GG = ganglioglioma; HA = hippocampal atrophy; HS = hippocampal sclerosis; ISCH = ischemia; SE = status epilepticus; SGL = subgranular layer; SVZ = sub-ventricular zone; TLE = temporal lobe epilepsy; VEGF = vascular endothelial growth factor; ZO-1 = zonula occludens-1.

Received December 29, 2006. Revised April 12, 2007. Accepted April 30, 2007. Advance Access publication May 28, 2007

Introduction

The most common form of partial epilepsy, temporal lobe epilepsy (TLE) is often refractory to antiepileptic drugs, but can be treated by surgical resection of the focus (Engel, 2001). Mesial temporal lobe epilepsy (MTLE), which represents more than 60% of TLE, is associated with hippocampal sclerosis (HS) characterized by severe neuronal loss and intense gliosis. In a previous study on tissue remodelling in MTLE, we described abundant neural progenitors in three areas, the sub-granular layer (SGL),

the subventricular zone (SVZ) and the fissura hippocampi (FH) (Crespel *et al.*, 2005). Surprisingly, we observed numerous vascular progenitor-like cells in the same areas. Moreover, in the dispersed granular layer many long microvessels, originating from the SGL, paralleled the radial astrocytic scaffolding (Crespel *et al.*, 2002). These observations suggested that a vascular remodelling occurred in MTLE. At the beginning of 20th century, vascular dysfunction was proposed to be a causal factor for MTLE or for HS (Bratz, 1899; Spielmeyer, 1927), but this hypothesis was later ruled out, due to the increased local blood flow during seizures (Gibbs, 1934). Recently, functional impairments of the vasculature and the blood–brain barrier (BBB) were reported in MTLE, such as a deficit in the control of homoeostasis by aquaporin (Eid *et al.*, 2005) or leakage of serum albumin (Van Vliet *et al.*, 2007). The latter was shown to be epileptogenic (Seiffert *et al.*, 2004; Ivens *et al.*, 2007). Nevertheless, all studies on human epileptic tissue concerned exclusively MTLE. The vascularization was not examined in TLE patients with aetiologies other than HS, even though these forms do not clearly differ from MTLE in terms of semiology and sensitivity to anti-epileptic drugs. They all present similar variations of cerebral blood flow and metabolism (Duncan, 1997; Oommen *et al.*, 2004), suggesting that haemodynamic changes are related to the epileptic activity *per se* and not to the neuropathological substrate.

The present study in adult patients suffering from intractable TLE with various aetiologies was designed to investigate: (i) vascular remodelling, (ii) the expression of angiogenic factors and tyrosine kinase receptors, (iii) a possible impairment of the BBB. In parallel, we looked for similar modifications during the development of epilepsy in the rat model of lithium-pilocarpine-induced status epilepticus (SE) which generates a chronic limbic epilepsy (Turski *et al.*, 1989).

Subjects, materials and methods

Subjects and clinical data

This study was in accordance with French Ethical Committee and received the approval of the Comité National Informatique et Libertés. All patients (or their families) were informed of additional studies performed on surgical tissue and provided a written consent. Tissue was obtained and used in a manner compliant with the Declaration of Helsinki.

All patients suffered from intractable partial complex seizures and the epileptic focus was localized on the temporal lobe, as revealed by neurological examination, long-term EEG-video-monitoring and morphological MRI to detect HS, defined by T2 hyper signal and decrease of hippocampal volume. They had a right or left classical TLE, except for one patient who showed an external temporal lobe focus. All patients underwent blood flow studies with 99mTc-HMPAO-single photon emission computed tomography (SPECT), during periictal and interictal periods. All clinical data are detailed in Table 1. Surgery consisted of anterior temporal lobectomy with amygdalo-hippocampectomy made by the same neurosurgeon for all epileptic patients. Several samples of each hippocampus were either rapidly frozen in liquid nitrogen or fixed by immersion in 10% buffered formalin and processed into liquid paraffin for histological evaluation and immunohistochemistry. The temporal poles were directly frozen in liquid nitrogen.

Two hippocampal control specimens were obtained during tumour surgery of non-epileptic patients and were processed in a similar way to the surgical specimens mentioned earlier. These patients had no history of epileptic seizures but suffered from either an anaplastic oligoastrocytoma (WHO grade III, $n=1$) or pilocytic astrocytoma (WHO grade I, $n=1$) adjacent to the hippocampal formation. Histological examination excluded tumour cell invasion or other neuropathological alterations within the hippocampal formation. Samples of hippocampi were rapidly frozen or fixed by immersion in 10% formalin.

In addition, three specimens from autopsied adult patients without neurological disorders were used as controls. The post-mortem intervals ranged from 24 to 48 h. The tissues were immersion-fixed for at least 1 month in 10% formalin and samples were embedded in paraffin. None of these patients had clinical evidence of neurological disease and the brains were normal as confirmed by a thorough neuropathological examination. For the Western blot study, we selected a high-grade brain tumour (glioblastoma) as a positive control for angiogenesis.

Rat model of limbic epilepsy

All animal procedures were conducted in accordance with the European Communities Council Directive of November 24, 1986 (86/609/EEC) and approved by the French Ministry of Agriculture (authorization no. 34178, M.L-N).

Surgery: 60 male Sprague–Dawley rats (Janvier, Le Genest-St-Isle, France), weighing 200–250 g at surgery were anaesthetized intraperitoneally (i.p.) with 3 ml.kg^{-1} of Equithesin and prepared for surgery, using a David Kopf stereotaxic apparatus. A deep bipolar electrode (made of 2 strands of 100 µm nickel chrome insulated wires twisted together) was implanted in the right hippocampus with the following coordinates: anterior to lamda: 4, lateral to lambda: 2.5, inferior to lambda: 2.5). Two extradural screws were inserted bilaterally in the parietal bone and one in the frontal bone (ground electrode). Deep electrodes and screws were linked to a microconnector fixed to the skull with acrylic cement.

One week post-surgery, rats were injected with lithium (3 meq.kg^{-1} i.p., Sigma, Saint-Louis, MO). Approximately 18 h later, methylscopolamine bromide (1 mg.kg^{-1} i.p., Sigma, Saint-Louis, MO) was administered to limit the peripheral effects of the convulsant. Thirty minutes later, status epilepticus (SE) was induced by injecting pilocarpine hydrochloride (30 mg.kg^{-1}, i.p., Sigma, Saint-Louis, MO) in 42 rats. Animals were put into individual boxes and their microconnectors were connected to an EEG preamplifier box (Reega mini8, Alvar, Montreuil, France). The electrical activity, recorded by deep and extradural electrodes, was filtered by a computer equipped with Dasylab software (Moenchengladbach, Germany).

For each animal, limbic seizures were recorded and observed 15–20 min after pilocarpine administration. They progressed rapidly to SE, characterized by continuous discharges on the EEG and partial as well-generalized seizures. Two hours after SE onset, we reduced the severity of convulsions with 2 mg.kg^{-1} diazepam i.p. (Roche, Neuilly, France), but limbic discharges

Table 1 Clinical data

Epileptic patients	Gender/age (y)	Side/type of epilepsy	Age at epilepsy onset (y or m)	Age at FS	Delay FPS-S (y)	Seizure frequency (*n*/month)	Aetiology	Perfusion ictal/interictal	Post-surgical outcome
P1	F/23	L TLE	7 y.	18 m.	16	5	HS	+/−	1A
P2	F/19	LTLE	7 y.	9 m.	12	5	HS	+/−	1A
P3	F/33	RTLE	28 y.	NO	5	5	HA	+/−	2A
P4	F/34	RTLE	23 y.	NO	11	3	HS	+/−	1A
P5	M/19	RTLE	3 y.	18 m.	16	5	HS	+/−	1A
P6	F/51	RTLE	13 y.	6 y.	38	5	HS	+/−	3A
P7	F/22	LTLE	4 y.	9 m.	18	9	HS	+/−	2A
P8	M/14	RTLE	12 y.	NO	2	3	DNET	+/−	1A
P9	M/26	LTLE	12 y.	NO	14	3	CRYPTO	+/−	1A
P10	F/47	RTLE	13 y.	NO	34	5	HA	+/−	2D
P11	M/33	L EXT.TLE	7 y.	NO	26	3	DNET	+/−	2B
P12	F/53	RTLE	41 y.	NO	12	10	HS	+/−	1A
P13	F/26	LTLE	18 y.	NO	8	1	DNET	+/−	1A
P14	F/22	LTLE	14 y.	NO	8	20	CRYPTO	+/−	1A
P15	M/35	LTLE	3 y.	12 m.	32	0.3	HA	+/−	1C
P16	M/30	RTLE	7 y.	NO	23	10	HS	+/−	1A
P17	F/32	RTLE	3 m.	NO	32	3	DYSP	+/−	1A
P18	M/17	RTLE	8 y.	3 y.	9	3	HS	+/−	1A
P19	F/39	RTLE	12 y.	NO	27	8	GG	+/−	1A
P20	M/47	RTLE	10 y.	NO	37	2	CRYPTO	+/−	1A
P21	M/28	LTLE	11 v	NO	17	5	HS	+/−	1A
P22	M/47	LTLE	13 m.	13 m.	46	3	HS	+/−	1A
P23	M/23	RTLE	11 y.	10 m.	12	4	HS	+/−	1A
P24	F/59	LTLE	38 y.	NO	21	3	AVM	+/−	1A
P25	M/42	RTLE	13 y.	NO	29	3	ISCH	+/−	4A
P26	M/30	RTLE	22 y.	9 m.	8	4	HS	+/−	1A
P27	F/27	RTLE	18 y.	NO	9	5	CRYPTO	+/−	1A
P28	M/47	LTLE	30 y.	NO	17	0.8	DYSP	+/−	1A
Control patients		Origin							
P29	M/20	Autopsy							
P30	M/47	Autopsy							
P31	M/31	Autopsy							
P32	F/8	Surgery							
P33	M/6	Surgery							

Note: F or M: female or male. L or R TLE: left or right temporal lobe epilepsy. Ext TLE: external temporal lobe epilepsy. Delay FPS-S: delay between first partial seizure and surgery. Aetiologies: HS: hippocampal sclerosis; HA: hippocampal atrophy; DNET: dysembryoplastic neuroepithelial tumour; DYSP: focal dysplasia; GG: ganglioglioma, AVM: arterio-venous malformation, ISCH: ischaemia, CRYPTO: cryptogenetic. Engel's classification: Ia: Fully seizure free since surgery. Id: Free disabling seizures but generalized convulsion antiepileptic drug withdrawal. 2a: Initially free of disabling seizures but rare seizures now. 2b: Rare disabling seizures since surgery. 3: Worthwhile improvement. 4a: No worthwhile improvement, some seizure reduction.

persisted on the EEG for several hours and rats exhibited partial seizures, similarly to what was reported by Andre *et al.* (2000). Eighteen control rats received the same treatment with lithium and methylscopolamine, but we used saline instead of pilocarpine. In previous experiments we and others (Andre *et al.*, 2000) compared EEG, behaviour and histology of naive and lithium-treated animals and we found no difference.

Rats were sacrificed at various time-points after the onset of SE, after an i.p. injection of 5 mg.kg^{-1} diazepam (Roche, Neuilly, France). Except for rats sacrificed in the acute period, others were recorded twice a week and we checked for interictal spikes or spontaneous seizures. Seizure recording on EEG was the only criterion to distinguish silent and chronic periods. Eleven rats died in the first week following SE. The number of animals used in this study was: for acute period, between 1 and 12 h after SE ($n = 13$), for silent period, from 4 to 14 d after SE ($n = 11$); for chronic period, between 21 and 28 d ($n = 7$). Sham-injected rats were sacrificed at similar time-points: controls for acute period: 1–3 h ($n = 4$); controls for silent period: 7–14 d ($n = 7$); controls for chronic period: 21–28 d ($n = 7$).

Histology, histochemistry and immunohistochemistry

Tissue processing

Human samples: formalin-fixed, paraffin-embedded 4-µm thick hippocampal sections were deparaffinized, and re-hydrated before histological evaluation and immunohistochemistry. For particular protocols without aldehyde fixation, frozen tissue was cut in a cryostat in 15 µm coronal sections.

Animal model: at various time-points after SE or sham injection, rats were sacrificed by decapitation after i.p. administration of 4 mg.kg^{-1} diazepam (Roche, Neuilly, France) to induce

relaxation. For standard morphological and immunohistochemical studies, brains were fixed by immersion in 4% paraformaldehyde in 0.1 M phosphate buffer and cut with a vibratome (30 µm coronal sections). For other studies, hemispheres were separated after decapitation, one was directly frozen in nitrogen, then cut with a cryostat (15 µm coronal sections) and the other was dissected to collect the hippocampus which was frozen for protein extraction (see Western blot protocol).

Histological diagnosis

For all patients, haematoxylin-eosin (HE) staining, performed on four sections at different levels of anteriority, allowed to confirm the aetiologies. All hippocampi from patients with HS diagnosed by MRI corresponded to the histological definition of HS: shrinkage, almost complete loss of neurons from the CA1, CA3 and end folium subfields, with relative sparing of CA2 and dentate granule cells and astrocytosis in lesioned subfields (HS, $n = 13$). The histological diagnosis in the other patients included focal hippocampal atrophy corresponding to a loss of volume (not diagnosed by T2 on MRI) with partial neuronal loss in CA1 and CA4 subfields (HA, $n = 3$), dysembryoplastic neuroepithelial tumour (DNET, $n = 3$), ganglioglioma (GG, $n = 1$), focal dysplasia (DYS, $n = 2$), arterio-venous malformation (AVM, $n = 1$), parahippocampal ischaemia (ISCH, $n = 1$) and cryptogenetic with normal histology (CRYPTO, $n = 4$).

For rats, Nissl or HE staining provided a way of detecting neuronal loss and granule cell dispersion.

Histochemical detection of vessels

Three techniques were used to easily stain the vasculature of human or rat hippocampi: (i) direct incubation of fixed sections in 3′,3′diaminobenzidine which reveals the endogenous peroxidase of red blood cells; (ii) direct staining of human or rat IgGs with species-specific antibodies (Table 2) conjugated either to fluorochrome or peroxidase; this technique allows to stain both microvessels and IgG accumulation in the parenchyma in case of BBB disruption; (iii) incubation with the biotin-conjugated *Bandeira simplicifolia* isolectin B4, revealed either by Texas Red-conjugated avidin or avidin–peroxidase complex (Vector, Burlingame, CA). After peroxidase detection using 3′,3′diaminobenzidine as a chromogen, sections were counterstained with Nissl, haematoxylin or HE.

Immunohistochemistry

For human sections, after quenching of endogenous peroxidase, an antigen retrieval was performed by immersion in citrate buffer, pH = 6 and heating (40 min at 100°C). The primary antibodies and their dilutions are listed in Table 2. Biotinylated secondary antibodies were raised against rabbit, goat or mouse IgGs at 1/500. All immunoperoxidase reactions were performed using avidin–biotin method and 3′,3′diaminobenzidine as chromogen. For human tissue, this method was performed with the Venting automatic immunoassaying system (Ventana Nexes, AR). For double labelling, a second staining was performed with avidin-alcaline phosphatase and revealed with Fast Red (Ventana Nexes, AR). Sections were finally counterstained with haematoxylin.

For immunofluorescence in human and animal tissue, we used secondary antibodies raised against rabbit, goat or mouse IgGs, conjugated to Cy3 (Jackson Immunoresearch, West Grove, PA) Alexa488 or Alexa647 (Molecular Probes, Eugene, OR), at 1/2000 dilution.

For the detection of Zonula Occludens-1 (ZO-1) a marker of tight junctions, a specific protocol was necessary in human and rats: without aldehyde fixation, 15 µm frozen sections were fixed in cold methanol for 5 min at 4°C. Then a double fluorescence labelling with ZO-1 antibody and lectin was performed.

Microscope observation and image acquisition

Nissl or HE staining, immunohistochemistry revealed by peroxidase or fluorescence were observed with a Leitz DMRB microscope (Leica, Wetzlar, Germany) equipped for epifluorescence (with tight filter bands centred on the peaks of emission of Alexa Fluor488, Cy3/Texas Red, Alexa Fluor350) and digitized by a 1392×1040 resolution cooled CCD camera (Cool Snap, Princeton Instrument, Trenton, NJ) on a computer using Cool Snap program and transferred to Adobe Photoshop (version 7) for image processing.

Rat double-labelled sections were observed using a confocal microscope (Zeiss 510 Meta, Göttingen, Germany) equipped with an ×25 objective (multi-immersion, numeric opening 0.8) and an ×63 objective (oil, numeric opening 1.4). We used an argon laser (excitation 488, emission 505–530 nm) for Alexa488, a helium laser (excitation 543, emission 585–615 nm) for Texas Red and a krypton-argon laser (excitation 647 nm, emission 660–700 nm) for Alexa647. Images were collected sequentially to avoid cross-contamination between fluorochromes. Series of 15 optical sections were projected onto a single image plane and scanned at 1024×1024 pixel resolution.

Western blot

Human tissue: Immediately after surgery, hippocampi and temporal poles were frozen in nitrogen and stored at −80°C. Samples were dissected, mechanically dissociated and homogenized in lysis buffer containing Tris (50 mM), EGTA (1 mM), sucrose (250 mM), non-ionic detergent Igepal (0.05%, Sigma Aldrich, St Quentin Fallavier, France), ionic detergent sodium deoxycholate (0.25%, Sigma Aldrich, St Quentin Fallavier, France) and protease inhibitor mixture (Roche Diagnostics, Meylan, France). After 10 min incubation at room temperature, samples underwent centrifugation for 15 min at 14 000 rpm at 4°C.

Rat tissue: Hippocampi were frozen and stored at −20°C immediately after dissection. They were mechanically dissociated and homogenized in a lysis buffer containing Tris (50 mM), EGTA (1 mM), sucrose (250 mM), phosphatase inhibitors (10 mM sodium fluoride and 1 mM orthovanadate) and protease inhibitor mixture. Samples underwent centrifugation for 10 min at 2300 rpm at 4°C. The supernatant was centrifuged at 37 000 rpm at 4°C for 30 min. Then the supernatant with soluble proteins was stored and membrane proteins in pellet were re-suspended in solubilization buffer containing Tris (50 mM), EDTA (1 mM), phosphatase inhibitors (10 mM sodium fluoride and 1 mM orthovanadate) and protease inhibitor mixture (Roche Diagnostics, Meylan, France).

Protein concentration was determined by using a BCA-Kit assay (Sigma, Saint-Louis, MO). Samples of 50 µg of protein boiled in Laemmli buffer were loaded onto a 12.5% acrylamide gel, separated electrophoretically and transferred to

Table 2 Primary antibodies and vascular markers

Primary antibodies	Source	Isotype	Clone or reference	Dilution	Supplier	IHC	WB
Glial fibrillary acidic protein (GFAP)	Mouse monoclonal	IgGI kappa	6F2	1/500 DAKO	DAKO Glostrup Denmark	+	
NeuN	Mouse monoclonal	IgGI	MAB377	1/500	CHEMICON Temecula CA	+	
Vascular Endothelial Growth Factor (VEGF)	* Rabbit polyclonal	IgG	Sc-507	1/200	Santa Cruz	+	
	* Mouse monoclonal	IgG	Sc-7269	1/100	Biotechnology		+
	* Goat polyclonal	IgG	Sc-1836	1/200	Santa-Cruz CA	+	+
CD31 (PECAM1)	Mouse monoclonal anti-human	IgGI kappa	JC70A	1/20	DAKO Glostrup Denmark	+	
Vimentine	Porcine monoclonal	IgGI	V9	1/6 Ready-to-use	Immunotech Temecula CA	+	
Von Willebrand Factor	Mouse monoclonal	IgGI kappa	F8/86	1/50	DAKO Glostrup Denmark	+	
Ki67	Mouse monoclonal	IgGI kappa	MIB1	1/100	DAKO Glostrup Denmark	+	
Neurofilaments	Mouse monoclonal	IgGI kappa	2F11	1/100	DAKO Glostrup Denmark	+	
Flk-1	Rabbit polyclonal	IgG	Sc-504	1/200	Santa Cruz	+	
				1/600	Biotechnology Santa-Cruz CA		+
Tie-2	Rabbit polyclonal anti-mouse	IgG	Sc-324	1/200	Santa Cruz	+	
				1/600	Biotechnology Santa-Cruz CA		+
Zonula Occludens 1 (ZO-1)	Rabbit polyclonal anti-human	IgG	61-7300	1/200	Zymed San Fransisco CA	+	
actin	Mouse monoclonal	IgG	ACTN05	1/1000	LabVision Fremont CA		+
OTHER MARKERS							
lectin	Biotinylated Isolectin B4		L-3759	1/200	SIGMA-ALDRICH St Quentin Fallavier-France	+	
Human IgG	Mouse biotinylated monoclonal	IgG	A57H	1/100	DAKO Glostrup Denmark	+	
Rat IgG	*Goat Alexa488 coupled Polyclonal	IgG	O-6382	1/2000	Molecular Probes Eugene OR	+	
	*Rabbit biotinylated polyclonal	IgG	BA-4001	1/100	Vector Labs Burlingame, CA	+	

polyvinyldifluoridine membranes (Hybond-C-extra, Amersham Biosciences, UK). Membranes were incubated 2 h in Tris buffered saline + Tween 5% (TBST) containing 5% skimmed milk, then overnight at 4°C with the following antibodies diluted in TBST + milk: VEGF, Flk-1, Tie-2 or Actin (see Table 2 for source and dilution). After washes in TBST, the secondary incubation was performed during 2 h at room temperature with peroxidase-conjugated goat anti-rabbit or anti-mouse antibodies (Jackson ImmunoResearch Ann Arbor, ME) 1/4000 or rabbit anti-goat antibody 1/5000 (Chemicon Temecula, CA). After three washes, chemoluminescence detection reagents (Western Lightening, Perkin Elmer and MA) enabled visualization of peroxidase reaction products. To quantify VEGF expression in the rat model, Western blots were analysed by densitometry using Photoshop and ImageJ.

Data analysis and statistics

Vascularization of human hippocampi from three groups of patients (NE $n = 5$, TLE without HS $n = 9$, TLE + HS $n = 8$) was quantified as follows: for each patient, three sections cut at different levels of the septo-temporal axis were immunostained with an anti-Von Willebrand factor antibody. On the three sections, images centred either on pyramidal or granular layers were acquired at ×20 magnification in each area: CA1/2, CA3/4 and DG. The density of microvessel network was quantified

according to the point-counting method (de Paz and Barrio, 1985) which takes into account the number, size and tortuosity of all vessels. A 5×5 grid (total field: $0.08\,mm^2$) was superposed to the digitized image, the number of labelled vessels crossing the grid was counted by an independent experimenter and expressed as vascular density (in arbitrary units) for a $0.08\,mm^2$ area. For each patient, the values obtained from the three areas (CA1/2, CA3/4 and DG) in the three sections were pooled to obtain a mean value for the whole hippocampus. Individual data were represented on a histogram.

The values of vascular density in the three groups of patients were compared using the non-parametric Kruskall–Wallis test with Bonferroni correction. The Spearman correlation coefficient was used to check for relationship between vascular density and other clinical parameters: age, gender, duration of epilepsy and seizure frequency.

In order to evaluate the progression of the vascular network in the rat model, we quantified vascular density in the hippocampus of pilocarpine-treated rats and their age-matched controls sacrificed during acute, silent or chronic periods. Coronal sections were collected at three levels of the septo-temporal axis and stained with 3′,3′ diaminobenzidine and haematoxylin. For each animal, four images at ×1.25 magnification of the hippocampus (anterior, median, postero-dorsal, postero-ventral) were digitized. The surfaces of the hippocampus and of the surrounding lateral ventricle were measured using Photoshop and ImageJ (Fig. 6B). The ratio of surfaces: hippocampus/(hippocampus + ventricle) was used as an index of hippocampal shrinkage and ventricle dilatation of dorsal and ventral hippocampus. At each level (anterior, median, postero-dorsal, postero-ventral), images centred on CA1median, CA1lateral, CA3, CA4 and DG were acquired at ×5 magnification and digitized (Fig. 6B). The point-counting was made with a 5×5 grid (total field: $1\,mm^2$) by two independent experimenters. The score was expressed in arbitrary units of vascular density for a $1\,mm^2$ area. The values of vascular density in the four areas (CA1median + lateral, CA3, CA4 and DG) were weighed using the ratio described earlier to take into account the hippocampal shrinkage.

We looked for putative differences in vascularization of the anterior and posterior parts of the hippocampus by measuring anterior and posterior densities in each animal, compared between the different groups by the paired-sample Wilcoxon rank test.

To reveal differences in vascular density between pilocarpine-treated rats and age-matched controls all individual data were pooled (for each area and for the whole hippocampus) and compared at each period, using the Kruskal–Wallis test and Bonferroni correction.

For animal studies, we quantified Western blot analysis by measuring optical density and compared control and pilocarpine-treated rats with the Kruskal–Wallis test and Bonferroni correction.

Results

Vascularization of the hippocampus in human TLE

An increase in the density of the vascular network was observed in TLE patients, whatever their aetiology: the size of large vessels remained unchanged, but the microvessels appeared longer, more tortuous and numerous than in NE subjects in all hippocampal areas, particularly in the layers containing neuronal cell bodies (Fig. 1A). Moreover, in patients with TLE+HS, the microvessels appeared radially orientated in the dispersed granular layer. The histogram in Fig. 1B shows individual values of vascular density for the whole hippocampus. The comparison of groups of patients revealed significant differences between epileptic and non-epileptic subjects (NE versus TLE and NE versus TLE+HS, $P < 0.01$). There was no difference between either groups of epileptic patients (TLE versus TLE+HS) and no correlation was found between the vascular density and the intensity of damage (ranging from cryptogenetic TLE to TLE+HS). We found that the vascular density was correlated neither to age and gender of patients, nor to duration of epilepsy.

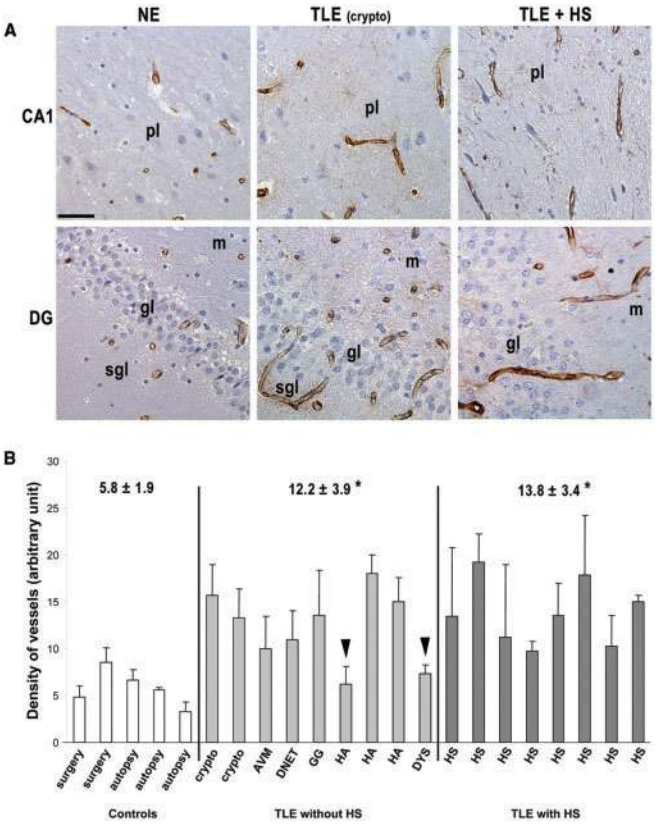

Fig. 1 Vascularization of the hippocampus in NE and TLE patients. (**A**) Immunohistochemical detection of Von Willebrand factor in CAI area and in dentate gyrus (DG). Anti-F8 antibody, Haematoxylin counterstaining. NE: non-epileptic patient, TLE (crypto): cryptogenetic temporal lobe epilepsy; TLE+HS: temporal lobe epilepsy with hippocampal sclerosis, pl: pyramidal layer, gl: granular layer, sgl: subgranular layer, m: dentate molecular layer. Scale bar: 50 μm. (**B**) Vascular density in the hippocampus was evaluated by the point counting method and expressed in arbitrary units for five NE patients, nine TLE patients with other aetiologies than HS and eight TLE patients with HS. Crypto: cryptogenetic, AVM: arterio-venous malformation, DNET: dysembryoplastic neuroepithelial tumour, GG: ganglioglioma, HA: hippocampal atrophy, DYS: focal dysplasia. Arrowheads show two TLE patients who had a very low seizure frequency. For each group of patients, mean and SEM were compared by Kruskall–Wallis test with Bonferroni correction. $^*P < 0.01$.

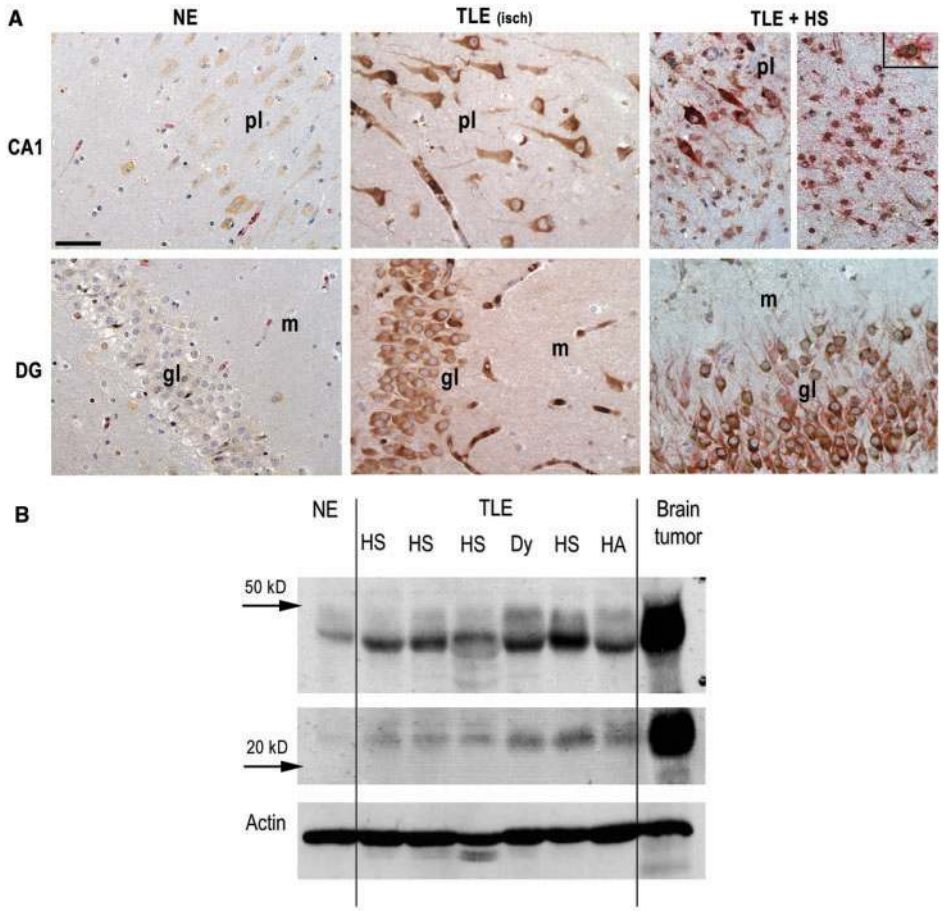

Fig. 2 VEGF expression in human TLE. (**A**) Immunostaining of VEGF (brown) and vimentin (red) in CAI and dentate gyrus from a non-epileptic patient (NE) and from two patients with TLE, either secondary to an ischaemic event (isch) or associated with hippocampal sclerosis (HS). Higher magnification: astrocyte positive for VEGF and vimentin. Haematoxylin counterstaining. pl: pyramidal layer, gl: granular layer, m: dentate molecular layer. Scale bar: 50 μm. (**B**) Detection on Western blot of the different isoforms of VEGF. NE: hippocampus surgically removed from a non-epileptic patient. TLE patients with various aetiologies; hippocampal sclerosis (HS) or hippocampal atrophy (HA) or focal dysplasia (Dy). A tumour tissue (glioblastoma) was used as a positive control for angiogenesis and actin antibody as a control of experimental variations.

Nevertheless, it was significantly correlated with the frequency of seizures (Spearman coefficient: 0.53, $P<0.05$). It is worth noting that two patients with less than one seizure per month (see arrowheads on Fig. 1B) showed a low density of vessels, while other patients with 1 to 20 seizures per month displayed similar increases in vascular density.

Expression of the vascular endothelial growth factor

We evaluated the expression of VEGF in the hippocampi of all TLE and NE patients. A basal level of VEGF expression was observed in neurons of control hippocampi, but in one NE patient (autopsy after suicide) the VEGF staining was very strong in CA1 pyramidal neurons. This demonstrates that these neurons are extremely sensitive to anoxia and that VEGF induction is rapid. Therefore, only for VEGF expression, the hippocampi obtained after ablation of para-hippocampal tumours under the same surgical conditions as for TLE patients, were used as controls.

In patients with TLE, pyramidal neurons and granule cells were strongly immunopositive for VEGF. Other cell types were also stained, but this expression seemed to depend on aetiology: in cases of TLE secondary to ischaemia or arterio-venous malformation, VEGF was highly expressed in vascular cells, whereas in all patients with HS, VEGF was present in reactive astrocytes of the CA1 area (Fig. 2A).

Western blot analysis was used to evaluate the expression of different isoforms of VEGF by their molecular weight. In human, we observed two isoforms, one at 46 kDa corresponding to the long form of VEGF165 and the other at 21 kDa corresponding to the short form of VEGF121 (Tee and Jaffe, 2001). A high grade tumour (glioblastoma) was used as a positive control for a maximal expression of VEGF isoforms. These results confirmed the slight basal level of VEGF in the hippocampus of NE patients and its

over-expression (both isoforms) in different TLE patients with either HS or other aetiologies (Fig. 2B). Patients with a low seizure frequency and a 'normal' vascularization had a moderate expression of VEGF, higher than NE patients (see the lane 'HA' on western blot).

Expression of tyrosine kinase receptors

The VEGF receptor 2 (VEGF-R2 or Flk-1) was expressed in very few vascular cells in the hippocampus of NE subjects; in TLE patients, Flk-1 immunostaining was obvious in all hippocampal areas, mainly on short, branched and sprouting collaterals of microvessels (Fig. 3A).

A similar staining pattern was observed for the angiopoietin receptor Tie-2, which is also crucial in angiogenesis and BBB integrity (Zhang and Chopp, 2002; Eklund and Olsen, 2006). Tie-2 was rarely detected in control tissues, whereas many Tie-2-positive cells were obvious in the hippocampi of all TLE patients, in vascular walls and sprouting collaterals. Moreover, a strong cytoplasmic Tie-2 staining was present in numerous single, small, round cells. They seemed to derive from highly vascularized areas (SVZ, FH) and to invade all hippocampal regions. In the vicinity of microvessels, some of them were grouped in clusters along the vascular walls (Fig. 3B). These Tie-2-positive cells were immunoreactive for CD31 (Fig. 3C) and lectin (not shown). Like for VEGF, the expression of both receptors did not differ depending on the aetiology of TLE (Fig. 3D).

Disruption of the blood–brain barrier

To evaluate the putative damage of the BBB, we looked for a leakage of serum IgGs using immunohistochemistry. In NE patients, IgGs were restricted to the inside of vessels (not shown), whereas in TLE subjects we observed an extravascular IgG staining in different areas. IgGs formed halos with a concentration gradient around vessels in the dentate granular layer and the hilus. In CA1/CA3 areas, IgG staining was widespread in the parenchyma. Surprisingly, the cytoplasm and dendrites of numerous pyramidal neurons were clearly immunoreactive for IgGs (Fig. 4A). Additionally, we checked for the expression of ZO-1, a marker of tight junctions, in only one patient with TLE; the immunostaining required a specific fixative protocol, we therefore could not use other samples. We observed an irregular and discontinuous expression of ZO-1 in microvessels identified by lectin (Fig. 4B).

Angiogenic processes in extra-hippocampal structures of the epileptogenic network

To address the question of vascular changes in extra-hippocampal structures, we looked for angiogenic factors and receptors in the temporal pole of TLE patients with different aetiologies. The levels of VEGF isoforms, of Flk-1 and of Tie-2, evaluated by Western blotting, were comparable to those measured in the hippocampus, without any correlation with the aetiology of TLE (Fig. 5A). Therefore, angiogenic factors seem to be highly expressed in extra-hippocampal structures which participate in the epileptogenic network. It is worth noting that haemodynamic variations affect the temporal pole as well as the hippocampus. These variations do not depend on damage, as illustrated by SPECT images of cerebral blood flow, in a patient with a cryptogenetic TLE (Fig. 5B).

Neuronal loss, shrinkage and neo-vascularization in the animal model of TLE

In rats, the lithium-pilocarpine injection induced a limbic, secondarily generalized status epilepticus. Neuronal loss affected many structures: hippocampus, amygdala, piriform and entorhinal cortices, thalamic nuclei and substantia nigra. Rats that experienced SE developed spontaneous seizures after 3–4 weeks (chronic period). At this time, neuronal loss was evident in pyramidal layers of CA1, CA3 and CA4, frequently associated with a severe dilatation of lateral ventricles surrounding the shrunken dorsal hippocampus. The surface ratio hippocampus/(hippocampus+ventricle) decreased gradually, mainly in dorsal hippocampus, reflecting a progressive shrinkage (around 10% at 1 week post-SE and $\geqslant$20% during the chronic period).

As shown in Fig. 6A, the vascular network increased in epileptic rats. There was no obvious difference in the density of vessels between rats sacrificed during SE and controls. During the silent period, microvessels appeared more numerous in the SVZ, FH and SGL; in the chronic period, their number, size and complexity were greatly increased in these areas and in the pyramidal and granular layers.

Quantification with the point-counting method revealed that rats showed an increase in vascular density during silent and chronic periods compared to age-matched controls ($P<0.01$ and 0.02 respectively) (Fig. 6C). Moreover, individual values were stronger in anterior than in posterior hippocampus, even after correction by the shrinkage ratio ($P<0.05$).

Angiogenic factors in the animal model of TLE

VEGF expression was studied in rat hippocampi during acute, silent and chronic periods (Fig. 7A). In control rats, neurons and astrocytes expressed a basal level of VEGF. During SE, some neurons showed a high level of VEGF likely stored in vesicle-like structures. During the silent period, both neurons and astrocytes strongly expressed VEGF in large vesicles. During the chronic period, the main source of VEGF was the high amount of hypertrophic, reactive astrocytes. Western blot analysis revealed two bands corresponding to long forms of VEGF165 (46 kDa) and VEGF121 (35 kDa) (Fig. 7B). The levels increased

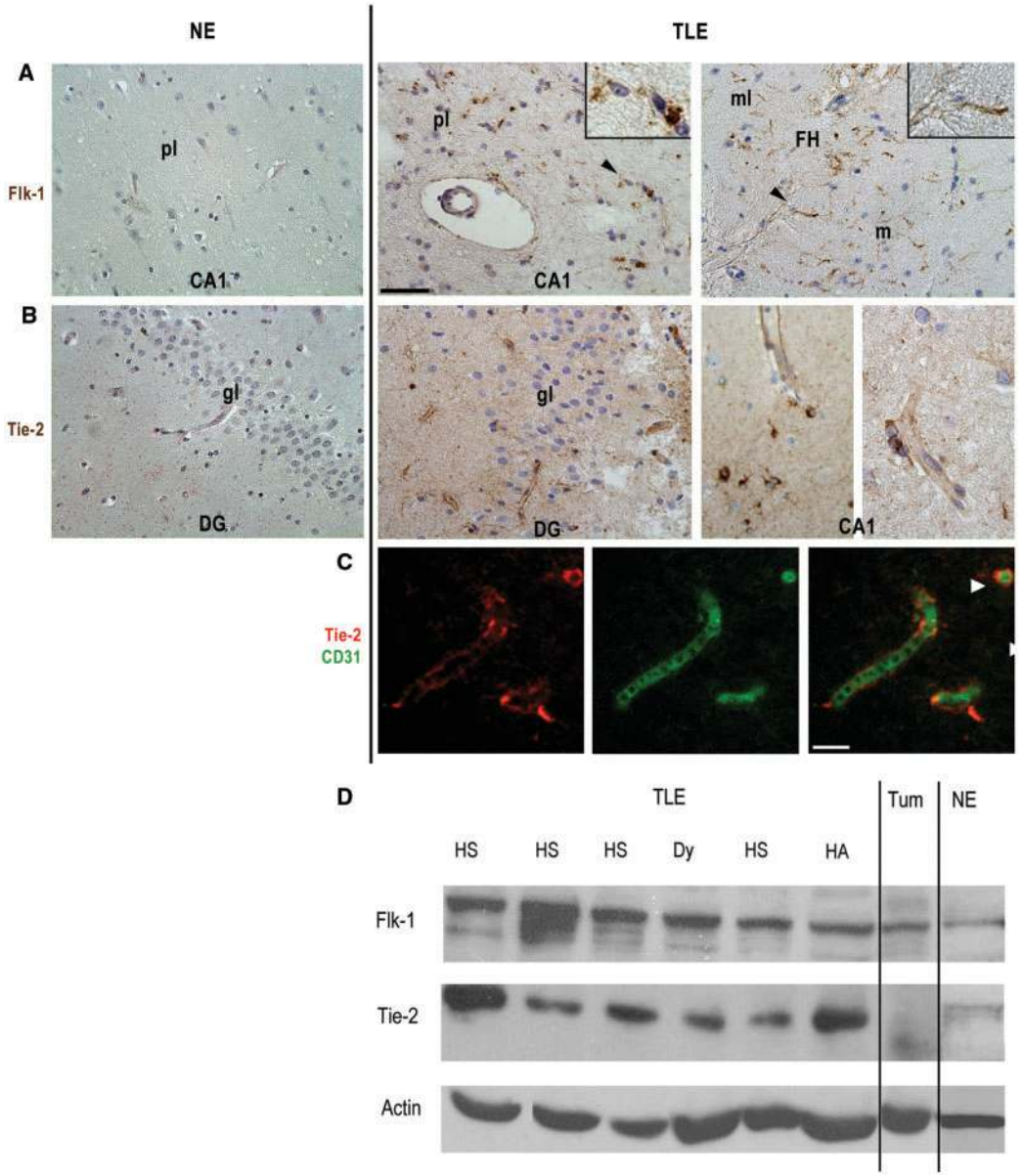

Fig. 3 Expression of receptors of angiogenic factors in Human TLE. Non-epileptic (NE, left) and epileptic patients (TLE, right). (**A**) Immuno-detection of Flk-1 (VEGF receptor-2) in thin sprouting collaterals, in CAI area or in the vicinity of the fissura hippocampi (FH) from TLE patients. Arrowheads indicate stained microvessels observed at higher magnifications. pl: pyramidal layer, ml: hippocampal molecular layer, m: dentate molecular layer. (**B**) Immunostaining of Tie-2 (angiopoietin receptor) in microvessels of the granular layer (gl) of the dentate gyrus (DG) and of the CAI area from TLE patients. Tie-2 is also expressed by small round cells, either single or arranged in clusters close to vessels. Scale bar: 50 μm for A and B (DG), 25 μm for B (CAI). Haematoxylin counterstaining. (**C**) Immunofluorescent detection of Tie-2 (left), CD3I (middle) and merge (right), suggesting that single Tie-2 positive cells are endothelial immature cells. Scale bar: 25 μm. (**D**): Western blot with antibodies against Flk-I and Tie-2. TLE patients with various aetiologies; hippocampal sclerosis (HS) or hippocampal atrophy (HA) or focal dysplasia (Dy). NE: hippocampus surgically removed from a non-epileptic patient. A tumour tissue (glioblastoma) was used as a positive control for angiogenesis and actin antibody as a control of experimental variations.

significantly in SE rats during the acute period compared to controls ($P<0.05$), decreased to basal levels in the silent period and slightly increased again during the chronic period (Fig. 7C).

BBB disruption in the animal model of TLE

The detection of extra-vascular IgGs (Fig. 8A) revealed a rapid BBB impairment after SE and, as for human TLE, a particular cytoplasmic staining in neurons. IgGs were first found in interneurons of the stratum oriens and the hilus during the acute period, then in numerous pyramidal neurons of CA1, CA3 and CA4, intensely during the silent period and at a lower level during the chronic period. Using an immuno-peroxidase detection of rat IgGs counterstained with HE, we superposed the brightfield image of IgGs and the fluorescent image of eosin.

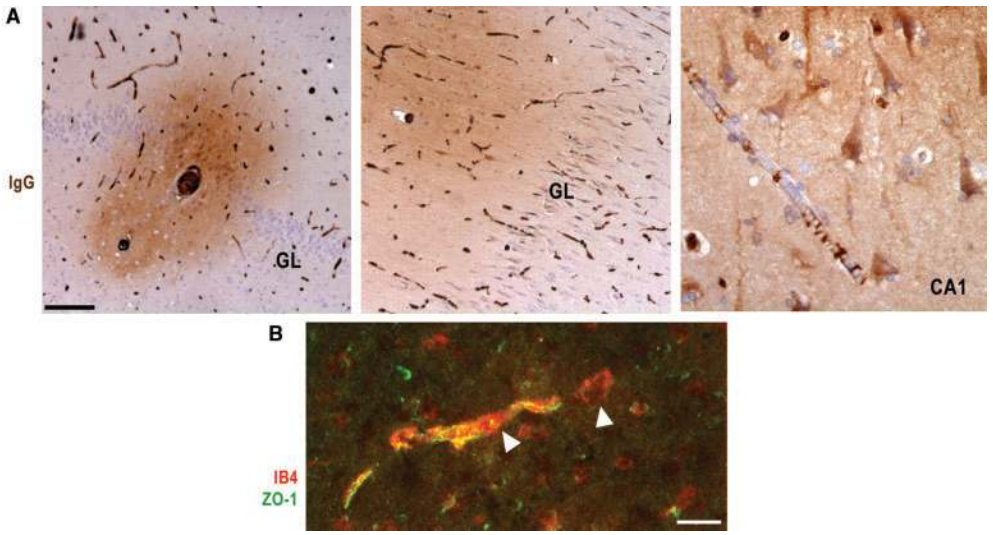

Fig. 4 Disruption of the blood–brain barrier in human TLE. (**A**) IgG leakage (anti-Human IgG antibody, Haematoxylin counterstaining). IgGs form halos around microvessels inside and under the granular layer (GL). In CA1, IgG staining is diffuse in the interstitial space and dense in the cytoplasm of pyramidal neurons. Scale bar: left and middle 200 μm, right 50 μm. (**B**) Loss of tight junctions. Immunostaining of zonula-occludens-1 (ZO-1, green) and labelling of vessels with isolectin B4 (IB4) in CA1 area. Scale bar: 15 μm.

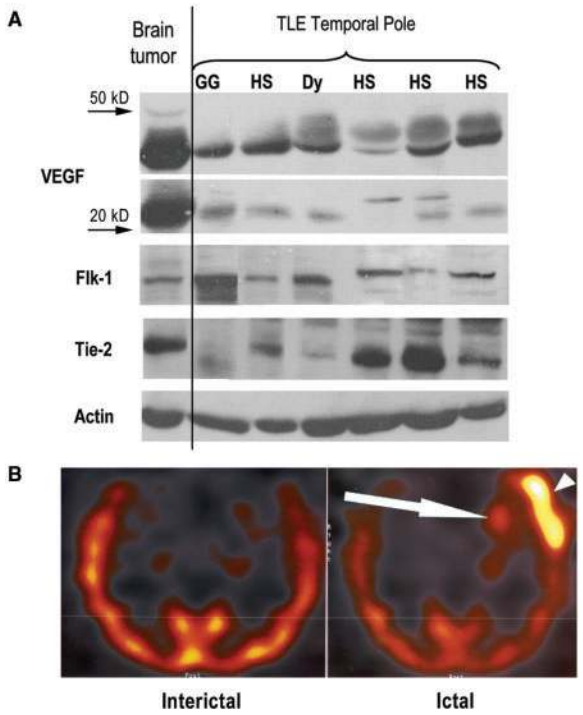

Fig. 5 Angiogenic processes and haemodynamic changes in extra-hippocampal structures of the epileptogenic network. (**A**) Expression of angiogenic factors and receptors in the temporal pole evaluated by Western blot with antibodies against VEGF (different isoforms), Flk-1 and Tie-2. Aetiologies were: hippocampal sclerosis (HS), focal dysplasia (Dy) or ganglioglioma (GG). A tumour tissue (glioblastoma) was used as a positive control and actin antibody as a control of experimental variations. (**B**) Cerebral blood flow measured by 99mTc-HMPAO-SPECT during interictal and ictal periods in a patient with cryptogenetic TLE. Arrows show the hippocampus and arrowheads the temporal pole: both are hyperperfused during seizures and hypoperfused in interictal periods.

We observed that most IgG-positive neurons were eosinophilic during silent and chronic periods. The loss of tight junctions was assessed by ZO-1 staining at all time-points. Hippocampal vessels of control rats showed a uniform staining of ZO-1 at inter-endothelial junctions, whereas 3 h after the beginning of SE and at later stages, the vascular ZO-1 staining was discontinuous (Fig. 8B).

Discussion

This study demonstrates for the first time an aberrant angiogenesis in chronic temporal lobe epilepsy, whatever the history of the disease or its morphological substrate. Using a relevant animal model of limbic epilepsy, we were able to provide evidence of some key events involved progressively in this vascular remodelling: (1) a transient up-regulation of VEGF in neurons after seizures, (2) the expression of tyrosine kinase receptors in microvessels, (3) an angiogenic sprouting, (4) the disruption of the BBB with a leakage of IgGs, (5) their uptake by neurons.

Causes of angiogenesis

Are seizures the trigger?

We postulate that angiogenesis observed in human TLE is not a consequence of excitotoxic processes or inflammatory reactions, but is induced by seizures *per se*. Our hypothesis is based on: (i) the massive up-regulation of VEGF in neurons after acute, short or long lasting seizures, described here and by others (Newton *et al.*, 2003; Croll *et al.*, 2004), (ii) the comparable increase in vascular density and the similar levels of angiogenic factors in TLE, whatever the aetiology or the extent of damage, (iii) the similar expression of VEGF and its receptors in the hippocampus,

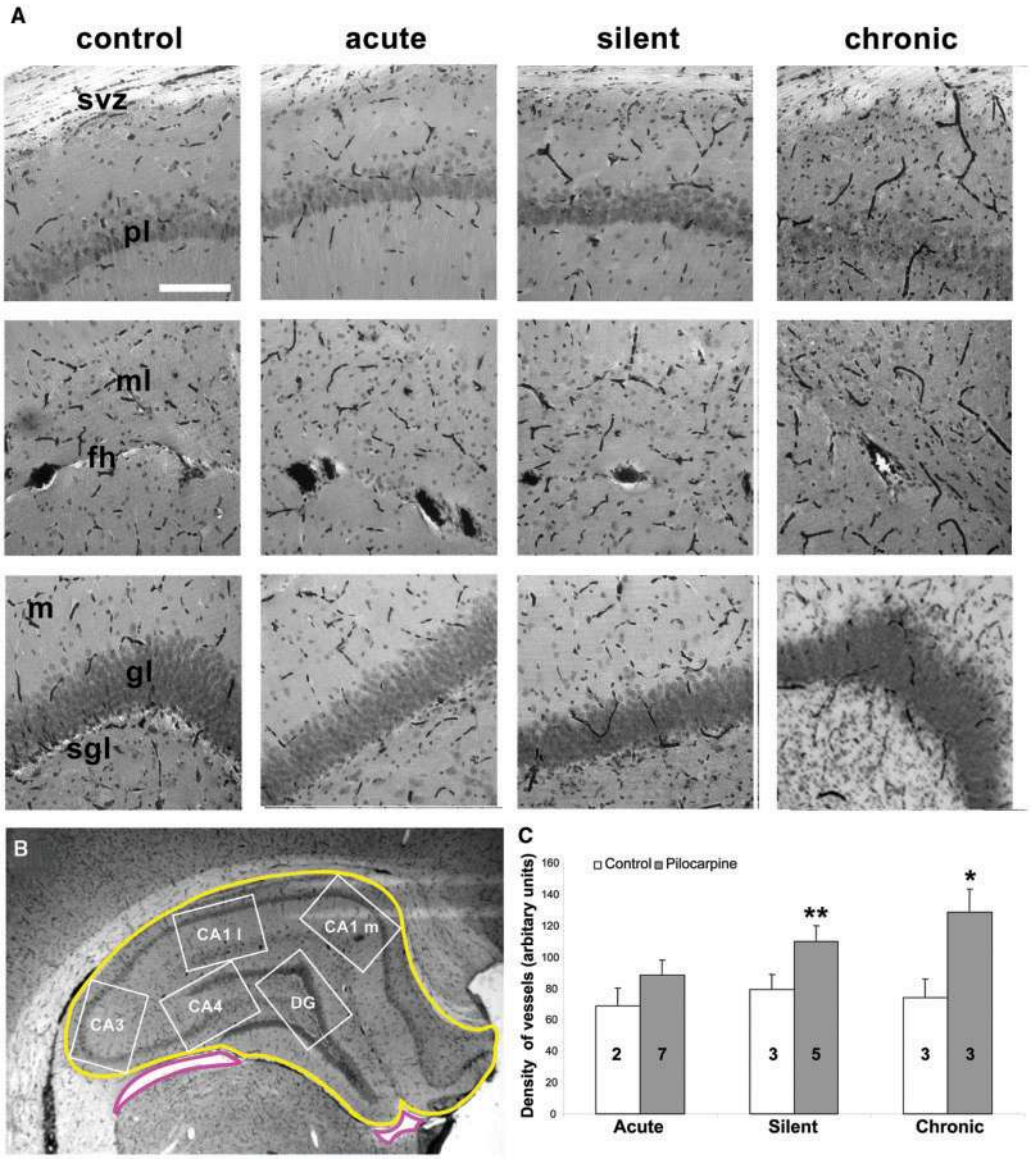

Fig. 6 Increased vascularization of the hippocampus in a rat model of limbic status epilepticus (SE) induced by lithium-pilocarpine. (**A**) Vascularization in different regions of the hippocampus in a control rat and rats sacrificed during acute, silent and chronic periods; upper images show the subventricular zone (svz) and the pyramidal layer (pl) of CA1, middle images the fissura hippocampi (fh) and the molecular layer (ml) of CA1, lower images the subgranular layer (sgl) the granular layer (gl) and the stratum moleculare (m) of the dentate gyrus. Detection of endogenous peroxidase by di-aminobenzidine, Nissl counterstaining, scale bar: 100 μm. (**B**) Schema superposed on a digitized image of the hippocampus, showing the hippocampal (yellow) and ventricular (pink) surfaces which were measured to evaluate the hippocampal shrinkage; white frames represent the position of the areas selected to quantify the density of vessels, as described in methods. (**C**) Means and SEM of vessel density in the hippocampus of rats sacrificed at different periods (acute, silent and chronic) after pilocarpine-induced SE and of age-matched controls. $^{*}P < 0.02$, $^{**}P < 0.01$, Kruskall–Wallis test, Bonferroni correction.

the primary focus and in the temporal pole cortex, a structure involved in the propagation of seizures (Chabardes *et al.*, 2005).

Once initiated, the angiogenic processes increase progressively, even in the absence of seizures as observed during the silent period, in the present study, or after single short seizures induced by electro-convulsive shock (Newton *et al.*, 2003; Hellsten *et al.*, 2005; Newton *et al.*, 2006). In the chronic period, the high expression of VEGF and tyrosine kinase receptors suggest that angiogenesis is either chronic or recurrently activated by spontaneous seizures. To support the second hypothesis, we found a positive correlation between seizure frequency and vascular density.

Up-regulation of VEGF and Flk-1

We suggest that the first step in the course of angiogenic events is the induction of VEGF by seizures. In rats, an up-regulation of VEGF in neurons and glia was described

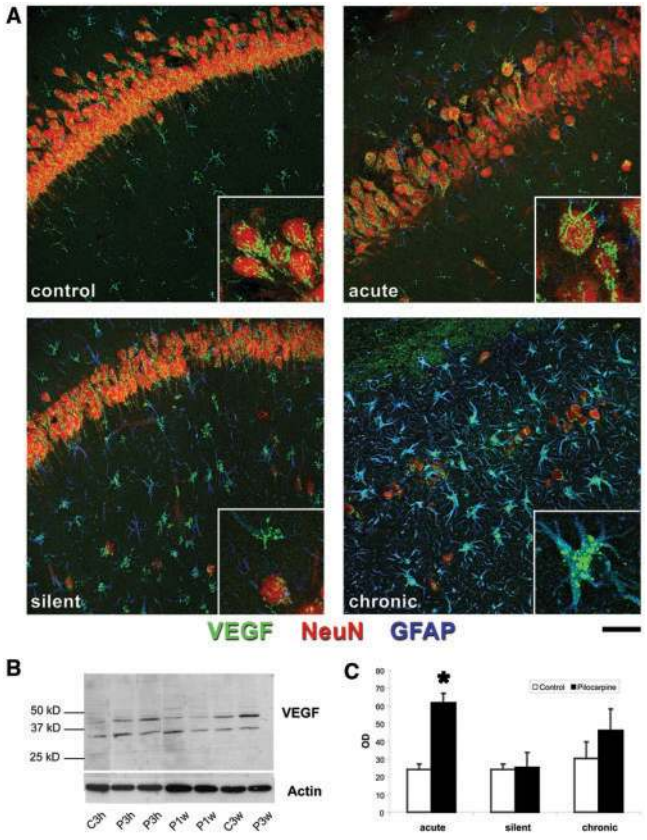

Fig. 7 VEGF expression in rats after limbic status epilepticus (SE). (**A**) Confocal images of immunostaining of VEGF (green), NeuN (red) and GFAP (blue) in the CA1 area of control and pilocarpine-treated rats sacrificed during acute, silent and chronic periods. The pyramidal layer is strongly labelled with the specific neuronal marker NeuN. Higher magnifications show neurons or astrocytes expressing VEGF in vesicle-like structures (green spots). Scale bar: 50 μm. (**B**) Western blot showing the different isoforms of VEGF at 3 h, 1 week and 3 weeks after pilocarpine-induced SE (P3h, P1w, P3w) and at 3 h or 3 weeks for control animals (C3h, C3w). The actin antibody was used as a control of experimental variations. (**C**) Quantification of Western blot analysis, expressed in optical density, comparing the VEGF expression in the hippocampus of pilocarpine-treated rats and age-matched controls at the three periods ($n = 2$ for each condition). $^*P < 0.05$. Kruskall–Wallis test, Bonferroni correction.

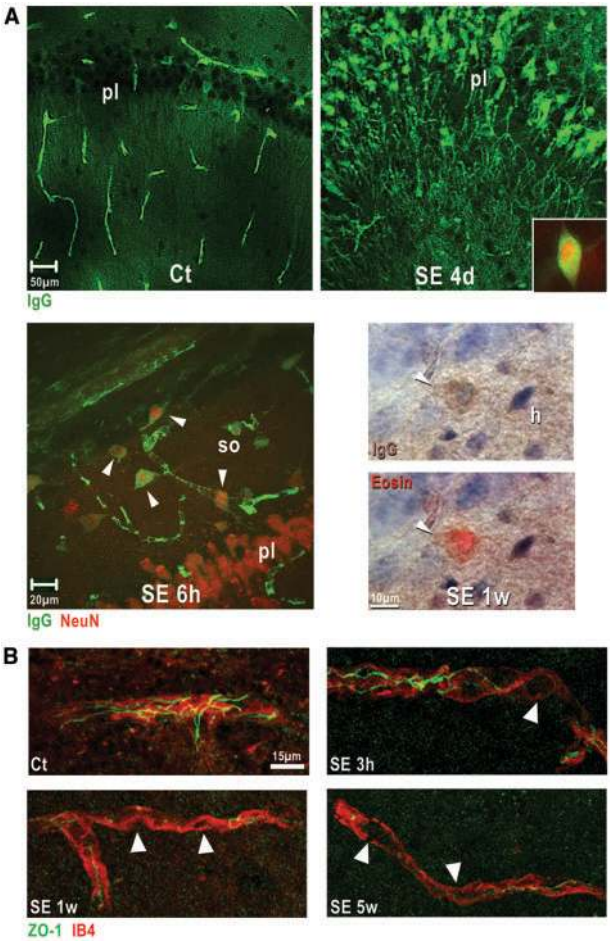

Fig. 8 Disruption of the blood–brain barrier in rats after limbic status epilepticus (SE). (**A**) IgG leakage and uptake by neurons at various time-points after SE. Ct and SE 4d: confocal images of IgG staining in vessels and in neurons in the CA3 area from a control rat and a rat sacrificed during the silent period (4 days after SE). Box: higher magnification of a CA3 pyramidal neuron double-labelled for IgG (green) and NeuN (red). SE 6 h: confocal image of the CA1 pyramidal layer (pl) and stratum oriens (so) of a rat sacrificed during the acute period (6 h of SE), stained for IgG (green) and NeuN (red); arrowheads indicate double-labelled interneurons. SE 1w: immunoperoxidase detection of IgG in the hilus of a rat sacrificed during the silent period (1 week post-SE) and superposition of the fluorescence emission of eosin; the arrowhead shows an interneuron which is IgG-positive and eosinophilic. (**B**) Confocal images of tight junctions, revealed by immuno-staining of zonula-occludens-1 (ZO-1, green) and labelling of vessels with isolectin B4 (IB4, red) in a control rat and at various time-points after SE. Arrowheads indicate the loss of tight junctions.

after SE by Croll *et al.* (2004). These authors proposed that hypoxia was the triggering factor, since the VEGF promoter contains a responsive element to the hypoxia-inducible factor (HIF) (Semenza, 2000). This is likely to be the case during a long-lasting SE. Nevertheless, VEGF can be also induced in response to intracellular signals of metabolic stress or to extracellular stimuli such as cytokines (Pages and Pouyssegur, 2005), that are known to occur in human and experimental seizures (Kann *et al.*, 2005; Vezzani and Granata, 2005).

In the chronic focus, we observed a strong VEGF expression by neurons in all cases of TLE. Glial or vascular expression of VEGF was rare and probably correlated with the aetiology: VEGF was observed in astrocytes in TLE with HS and in vascular cells in TLE associated with extra-hippocampal ischaemia or vascular malformation. In the rat model of TLE with neuronal loss and gliosis, we confirmed a progressive over-expression of VEGF by astrocytes. The levels of both isoforms of VEGF in the hippocampus or temporal pole of TLE patients compared to a high grade brain tumour suggested that the chronic focus is persistently exposed to a high concentration of VEGF. Even if

there are other factors released during seizures that participate in the neo-vascularization of the focus, the local concentration of VEGF is a pivotal actor that induces either a physiological or an aberrant angiogenesis (Ozawa *et al.*, 2004).

VEGF activates tyrosine kinase receptors expressed by different types of cells which promote both angiogenesis and neuroprotection (Storkebaum *et al.*, 2004). The angiogenic effects are mediated mainly by two receptors. VEGF-R2 (Flk-1) plays a crucial role in endothelial cell proliferation, migration and vascular development, whereas VEGF-R1 modulates proliferation. The neuronal Flk-1 seems to be the main effector of VEGF-induced neuroprotection through the activation the PI-3 kinase/Akt survival pathway (Kilic *et al.*, 2006). In adult rats, VEGF-R1 and VEGF-R2 are found on the surface of endothelial cells at very low levels. These receptors are both up-regulated at the surface of neurons and astrocytes after stroke (Lennmyr *et al.*, 1998). Here, we observed a specific staining of Flk-1 in sprouting microvessels only in TLE. We detected no Flk-1 in neurons or glia. This suggests that this expression is a transient protective mechanism after an ischaemic or epileptic event.

Up-regulation of Tie-2 receptor

Angiopoietin 1 and 2 (Ang1, Ang2) are known to play a role in physiological or post-ischaemic angiogenesis in synergy with VEGF (Zhang and Chopp, 2002). We detected no angiopoietins, but we were able to observe an intense expression of their Tie-2 receptor in chronic TLE. When activated by Ang1, Tie-2 terminates angiogenesis and improves vascular integrity, mainly via the PI-3 kinase pathway (Eklund and Olsen, 2006). On the contrary, Ang2 behaves as an antagonist (Bogdanovic *et al.*, 2006). Tie-2 staining was very scarce in NE patients and strong in short microvessels of all hippocampal areas in TLE patients, confirming the angiogenic sprouting. Moreover, Tie-2 was highly expressed by single cells, sometimes grouped in clusters along the vascular walls. Their localization and their phenotype is reminiscent of the recruitment of endothelial progenitor cells from peripheral circulation, which migrate to re-vascularize an ischemic tissue (Kopp *et al.*, 2006). Therefore, the high quantity of Tie-2 positive cells provides further evidence of the persistence of angiogenic processes in the chronic focus.

What are the consequences of angiogenesis in the epileptic focus?

Neuroprotection

Generally, the rapid secretion of growth factors after seizures is considered as a protective mechanism. This is the case for VEGF release, since its anti-epileptogenic and neuroprotective properties were recently demonstrated both *in vitro* and *in vivo* (McCloskey *et al.*, 2005).

Another effect of VEGF, that could be beneficial during seizures, is the fast adaptation of blood flow to the metabolic demand of neurons. VEGF, via the Flk-1/Akt pathway, activates the endothelial nitric oxide synthase (eNOS) which promotes immediate vasodilatation through NO release (Ahmad *et al.*, 2006). We previously showed that eNOS was over-expressed in microvessels of rat epileptic focus and that inhibiting NO synthesis dramatically worsened neuronal damage in kainate-induced SE (Rondouin *et al.*, 1993; Lerner-Natoli *et al.*, 1994).

Finally, the increased density of microvessels in the epileptic structures probably represents a progressive adaptation to improve perfusion during seizures. The ictal increase of both regional cerebral blood flow and metabolism during seizures, whatever aetiology or damage, is well-documented in humans (as illustrated in Fig. 5) and in different animal models (Lerner-Natoli *et al.*, 1983; Pinard *et al.*, 1987; Pereira de Vasconcelos *et al.*, 2002; Van Paesschen, 2004).

BBB impairment

If, after an acute event such as a stroke, angiogenesis contributes to tissue revascularization, persistent angiogenic processes are considered to be deleterious for brain tissue, mainly due to BBB permeability (Hayashi *et al.*, 2006). This is likely to be the case in chronic TLE and in different acute or chronic animal models of epilepsy. Single short seizures disrupt BBB (Goldman *et al.*, 1987; Devanand *et al.*, 1994; Oztas *et al.*, 2003) and seizure frequency is correlated to the degree of leakage (Van Vliet *et al.*, 2007). VEGF is known to play a main role in vascular permeability by activating matrix metalloproteases which break vessel walls (Hayashi *et al.*, 2006) and degrade tight junctions (Zhang and Chopp, 2002). Our study on the rat model showed that IgG leakage and ZO-1 decrease were obvious early after SE, but also during latent and chronic periods. Since angiogenic factors are recurrently up-regulated by seizures, proteolytic processes would persist and contribute to the chronic impairment of the BBB.

IgG leakage

The extravasation of IgGs and other serum proteins which accumulate in the cytoplasm of neurons has already been reported in the case of acute BBB breakdown, auto-immune or neurodegenerative diseases (Kitz *et al.*, 1984; Fabian and Petroff, 1987; Mori *et al.*, 1991; Loberg *et al.*, 1993; Orr *et al.*, 2005; Hallene *et al.*, 2006). We observed a neuronal uptake of IgGs in chronic TLE and the rat model showed that neurons were progressively affected in function of their vulnerability to seizures (first interneurons, then CA3/CA1 pyramidal neurons). An immune effect of IgGs on neuronal function has never been demonstrated in TLE, but the role of auto-antibodies in different forms of epilepsy is currently a matter of debate (McNamara, 2002; Watson *et al.*, 2004; Roubertie *et al.*, 2005). Nevertheless,

other serum proteins with no immune function are epileptogenic (Seiffert *et al.*, 2004). Recently, accumulation of albumin was described in the cytoplasm of neurons and astrocytes in human epilepsy or after an experimental BBB disruption (Van Vliet *et al.*, 2007). Its epileptogenic effect was demonstrated by Ivens *et al.* (2007) who showed that albumin uptake by astrocytes altered the potassium inward rectifying currents. Whether the accumulation of serum proteins in the interstitial space modifies oncotic pressure that contributes to vasogenic oedema and interictal hypoperfusion, remains to be elucidated.

Conclusion

The vascular remodelling described in this study is a common substrate for different forms of drug-refractory TLE and does not depend on their aetiologies. The hippocampus and other temporal structures of the epileptogenic network which show regional variations of blood flow are affected by neo-vascularization. Even if angiogenesis accounts for neuroprotective mechanisms during seizures, angiogenesis may be involved in the chronic permeability of the BBB with severe consequences, such as neurovascular uncoupling, inflammation and excitability. Future studies should focus on factors and signalling pathways involved in adult angiogenesis. By understanding the complex cross-talk between neurons, glia and endothelial cells, we may hope to develop novel therapeutic approaches of intractable epilepsy.

Supplementary Data

Supplementary Data is available at *BRAIN* online.

Acknowledgements

The authors are grateful to: Dr F. Bertaso for critically reading the manuscript, Dr G. Alonso for constructive discussions, A. Turner-Madeuf for language revision, L. Charvet for iconography and N. Lautredou-Audouy at the Centre Regional d'Imagerie Cellulaire for confocal microscopy. The technical assistance of L. Dumas, S. Lescure and D. Pierre in human histology was deeply appreciated. This study was supported by the French Foundation for Research on Epilepsy and the Foundation Thérèse and René Planiol for Research on Human Neuro-Vascular Pathologies.

References

Ahmad S, Hewett PW, Wang P, Al-Ani B, Cudmore M, Fujisawa T, et al. Direct evidence for endothelial vascular endothelial growth factor receptor-1 function in nitric oxide-mediated angiogenesis. Circ Res 2006; 99: 715–22.

Andre V, Ferrandon A, Marescaux C, Nehlig A. The lesional and epileptogenic consequences of lithium-pilocarpine-induced status epilepticus are affected by previous exposure to isolated seizures: effects of amygdala kindling and maximal electroshocks. Neuroscience 2000; 99: 469–81.

Bogdanovic E, Nguyen VP, Dumont DJ. Activation of Tie2 by angiopoietin-1 and angiopoietin-2 results in their release and receptor internalization. J Cell Sci 2006; 119: 3551–60.

Bratz E. Ammonshornbefunde bei Epileptikern. Arch Psychiatr Nervenkr 1899; 32: 820–35.

Chabardes S, Kahane P, Minotti L, Tassi L, Grand S, Hoffmann D, et al. The temporopolar cortex plays a pivotal role in temporal lobe seizures. Brain 2005; 128: 1818–31.

Crespel A, Coubes P, Rousset MC, Alonso G, Bockaert J, Baldy-Moulinier M, et al. Immature-like astrocytes are associated with dentate granule cell migration in human temporal lobe epilepsy. Neurosci Lett 2002; 330: 114–8.

Crespel A, Rigau V, Coubes P, Rousset MC, de Bock F, Okano H, et al. Increased number of neural progenitors in human temporal lobe epilepsy. Neurobiol Dis 2005; 19: 436–50.

Croll SD, Goodman JH, Scharfman HE. Vascular endothelial growth factor (VEGF) in seizures: a double-edged sword. Adv Exp Med Biol 2004; 548: 57–68.

de Paz P, Barrio JP. Stereological parameters from the analysis of the cell micrographs either by manual point-counting methods or by using a semi-automatic system: a BASIC program for ZX-spectrum personal computer. Comput Biol Med 1985; 15: 153–8.

Devanand DP, Dwork AJ, Hutchinson ER, Bolwig TG, Sackeim HA. Does ECT alter brain structure? Am J Psychiatry 1994; 151: 957–70.

Duncan JS. Imaging and epilepsy. Brain 1997; 120 (Pt 2): 339–77.

Eid T, Lee TS, Thomas MJ, Amiry-Moghaddam M, Bjornsen LP, Spencer DD, et al. Loss of perivascular aquaporin 4 may underlie deficient water and K+ homeostasis in the human epileptogenic hippocampus. Proc Natl Acad Sci USA 2005; 102: 1193–8.

Eklund L, Olsen BR. Tie receptors and their angiopoietin ligands are context-dependent regulators of vascular remodeling. Exp Cell Res 2006; 312: 630–41.

Engel J Jr. Mesial temporal lobe epilepsy: what have we learned? Neuroscientist 2001; 7: 340–52.

Fabian RH, Petroff G. Intraneuronal IgG in the central nervous system: uptake by retrograde axonal transport. Neurology 1987; 37: 1780–4.

Gibbs FL, Lennox WG, Gibbs EL. Cerebral blood flow preceding and accompanying epileptic seizure in man. Arch Neurol Psychiatr 1934; 32: 257–72.

Goldman H, Berman RF, Murphy S. ACTH-related peptides, kindling and seizure disorders. Adv Biochem Psychopharmacol 1987; 43: 317–27.

Hallene KL, Oby E, Lee BJ, Santaguida S, Bassanini S, Cipolla M, et al. Prenatal exposure to thalidomide, altered vasculogenesis, and CNS malformations. Neuroscience 2006; 142: 267–83.

Hayashi T, Deguchi K, Nagotani S, Zhang H, Sehara Y, Tsuchiya A, et al. Cerebral ischemia and angiogenesis. Curr Neurovasc Res 2006; 3: 119–29.

Hellsten J, West MJ, Arvidsson A, Ekstrand J, Jansson L, Wennstrom M, et al. Electroconvulsive seizures induce angiogenesis in adult rat hippocampus. Biol Psychiatry 2005; 58: 871–8.

Ivens S, Kaufer D, Flores LP, Bechmann I, Zumsteg D, Tomkins O, et al. TGF-{beta} receptor-mediated albumin uptake into astrocytes is involved in neocortical epileptogenesis. Brain 2007; 130: 535–47.

Kann O, Kovacs R, Njunting M, Behrens CJ, Otahal J, Lehmann TN, et al. Metabolic dysfunction during neuronal activation in the ex vivo hippocampus from chronic epileptic rats and humans. Brain 2005; 128: 2396–407.

Kilic E, Kilic U, Wang Y, Bassetti CL, Marti HH, Hermann DM. The phosphatidylinositol-3 kinase/Akt pathway mediates VEGF's neuroprotective activity and induces blood-brain barrier permeability after focal cerebral ischemia. Faseb J 2006; 20: 1185–7.

Kitz K, Lassmann H, Karcher D, Lowenthal A. Blood-brain barrier in chronic relapsing experimental allergic encephalomyelitis: a correlative study between cerebrospinal fluid protein concentrations and tracer

leakage in the central nervous system. Acta Neuropathol 1984; 63: 41–50.

Kopp HG, Ramos CA, Rafii S. Contribution of endothelial progenitors and proangiogenic hematopoietic cells to vascularization of tumor and ischemic tissue. Curr Opin Hematol 2006; 13: 175–81.

Lennmyr F, Ata KA, Funa K, Olsson Y, Terent A. Expression of vascular endothelial growth factor (VEGF) and its receptors (Flt-1 and Flk-1) following permanent and transient occlusion of the middle cerebral artery in the rat. J Neuropathol Exp Neurol 1998; 57: 874–82.

Lerner-Natoli M, de Bock F, Bockaert J, Rondouin G. NADPH diaphorase-positive cells in the brain after status epilepticus. Neuroreport 1994; 5: 2633–7.

Lerner-Natoli M, Le Ponçin-Laffite M, Rondouin G, Rapin J, Baldy-Moulinier M. Simultaneous determination of local cerebral blood flow and metabolism in the different stages of amygdala kindling. Cerebral blood flow, metabolism and epilepsy. London-Paris: John Libbey Eurotext; 1983.

Loberg EM, Karlsson BR, Torvik A. Neuronal uptake of plasma proteins after transient cerebral ischemia/hypoxia. Immunohistochemical studies on experimental animals and human brains. Apmis 1993; 101: 777–83.

McCloskey DP, Croll SD, Scharfman HE. Depression of synaptic transmission by vascular endothelial growth factor in adult rat hippocampus and evidence for increased efficacy after chronic seizures. J Neurosci 2005; 25: 8889–97.

McNamara JO. B cells and epilepsy: the odd couple. Neurology 2002; 58: 677–8.

Mori S, Sternberger NH, Herman MM, Sternberger LA. Leakage and neuronal uptake of serum protein in aged and Alzheimer brains. A postmortem phenomenon with antemortem etiology. Lab Invest 1991; 64: 345–51.

Newton SS, Collier EF, Hunsberger J, Adams D, Terwilliger R, Selvanayagam E, et al. Gene profile of electroconvulsive seizures: induction of neurotrophic and angiogenic factors. J Neurosci 2003; 23: 10841–51.

Newton SS, Girgenti MJ, Collier EF, Duman RS. Electroconvulsive seizure increases adult hippocampal angiogenesis in rats. Eur J Neurosci 2006; 24: 819–28.

Oommen KJ, Saba S, Oommen JA, Francel PC, Arnold CD, Wilson DA. The relative localizing value of interictal and immediate postictal SPECT in seizures of temporal lobe origin. J Nucl Med 2004; 45: 2021–5.

Orr CF, Rowe DB, Mizuno Y, Mori H, Halliday GM. A possible role for humoral immunity in the pathogenesis of Parkinson's disease. Brain 2005; 128: 2665–74.

Ozawa CR, Banfi A, Glazer NL, Thurston G, Springer ML, Kraft PE, et al. Microenvironmental VEGF concentration, not total dose, determines a threshold between normal and aberrant angiogenesis. J Clin Invest 2004; 113: 516–27.

Oztas B, Kaya M, Kucuk M, Tugran N. Influence of hypoosmolality on the blood-brain barrier permeability during epileptic seizures. Prog Neuropsychopharmacol Biol Psychiatry 2003; 27: 701–4.

Pages G, Pouyssegur J. Transcriptional regulation of the Vascular Endothelial Growth Factor gene–a concert of activating factors. Cardiovasc Res 2005; 65: 564–73.

Pereira de Vasconcelos A, Ferrandon A, Nehlig A. Local cerebral blood flow during lithium-pilocarpine seizures in the developing and adult rat: role of coupling between blood flow and metabolism in the genesis of neuronal damage. J Cereb Blood Flow Metab 2002; 22: 196–205.

Pinard E, Rigaud AS, Riche D, Naquet R, Seylaz J. Continuous determination of the cerebrovascular changes induced by bicuculline and kainic acid in unanaesthetized spontaneously breathing rats. Neuroscience 1987; 23: 943–52.

Rondouin G, Bockaert J, Lerner-Natoli M. L-nitroarginine, an inhibitor of NO synthase, dramatically worsens limbic epilepsy in rats. Neuroreport 1993; 4: 1187–90.

Roubertie A, Boukhaddaoui H, Sieso V, de Saint-Martin A, Lellouch-Tubiana A, Hirsch E, et al. Antiglial cell autoantibodies and childhood epilepsy: a case report. Epilepsia 2005; 46: 1308–12.

Seiffert E, Dreier JP, Ivens S, Bechmann I, Tomkins O, Heinemann U, et al. Lasting blood-brain barrier disruption induces epileptic focus in the rat somatosensory cortex. J Neurosci 2004; 24: 7829–36.

Semenza GL. Expression of hypoxia-inducible factor 1: mechanisms and consequences. Biochem Pharmacol 2000; 59: 47–53.

Spielmeyer W. Die Pathogenese des epileptisches Krampfes, histopathologischer Teil. Ztschr Neurol Psychiatr 1927; 109: 501–19.

Storkebaum E, Lambrechts D, Carmeliet P. VEGF: once regarded as a specific angiogenic factor, now implicated in neuroprotection. Bioessays 2004; 26: 943–54.

Tee MK, Jaffe RB. A precursor form of vascular endothelial growth factor arises by initiation from an upstream in-frame CUG codon. Biochem J 2001; 359: 219–26.

Turski L, Ikonomidou C, Turski WA, Bortolotto ZA, Cavalheiro EA. Review: cholinergic mechanisms and epileptogenesis. The seizures induced by pilocarpine: a novel experimental model of intractable epilepsy. Synapse 1989; 3: 154–71.

Van Paesschen W. Ictal SPECT. Epilepsia 2004; 45(Suppl 4): 35–40.

Van Vliet EA, Da Costa Araujo S, Redeker S, Van Schaik R, Aronica E, Gorter JA. Blood-brain barrier leakage may lead to progression of temporal lobe epilepsy. Brain 2007; 130: 521–34.

Vezzani A, Granata T. Brain inflammation in epilepsy: experimental and clinical evidence. Epilepsia 2005; 46: 1724–43.

Watson R, Jiang Y, Bermudez I, Houlihan L, Clover L, McKnight K, et al. Absence of antibodies to glutamate receptor type 3 (GluR3) in Rasmussen encephalitis. Neurology 2004; 63: 43–50.

Zhang Z, Chopp M. Vascular endothelial growth factor and angiopoietins in focal cerebral ischemia. Trends Cardiovasc Med 2002; 12: 62–6.